1996
doi:10.1017/S1431927613011975
Microsc. Microanal. 19 (Suppl 2), 2013


# Dynamical Control of Orbital Ordering and Ferroelectric-Induced Polar State in Metallic Manganites

Robert F Klie, Qiao Qiao, Ahmet Gulec, Patrick J. Phillips

Department of Physics, University of Illinois at Chicago

The breaking of orbital degeneracy on a transition metal cation and the resulting differing electronic occupations of these orbitals provide a powerful setting to control orbital energies, charge density, and spin ordering in complex oxides. We show that one can dynamically modulate the orbital polarization on the Mn atoms at ferroelectric/manganite interfaces by switching the ferroelectric polarization. The change in orbital occupation can be as large as 10%, greatly exceeding that of bulk manganites. In addition to Jahn-Teller-like distortions, this interfacial orbital polarization is also controlled by the propagation of the ferroelectric polar displacements into the interface region which represents a mechanism absent in the bulk and unique to the interface. We use *ab initio* theory, thin film growth techniques, and scanning transmission electron microscopy to verify the predicted interfacial polar state.

In this work, we grew heterostructures of 15 unit cells of $La_{0.8}Sr_{0.2}MnO_3$/20 unit cells of $BaTiO_3$/20 unit cells of $La_{0.8}Sr_{0.2}MnO_3$ on $TiO_2$-terminated substrates of $SrTiO_3$ (001). The heterostructures were grown in an ultra-high vacuum molecular beam epitaxy system at a base pressure of $1 \times 10^{-10}$ Torr. All high-angle annular dark-field (HAADF) and annular bright field (ABF) images, as well as electron energy loss (EEL) spectra shown in this study were acquired using the probe aberration-corrected JEOL JEM-ARM200CF at UIC, equipped with a 200 kV cold-field emission gun (CFEG), a post-column Gatan Enfina EEL spectrometer, and HAADF and ABF detectors. When operated at 200 kV, this microscope can achieve 0.35 eV energy and 73 pm spatial resolution, as shown in Figure 1. A 22 mrad probe convergence semi-angle was used and the detector inner angle for HAADF was 90 mrad, while the detector range for ABF imaging was 11-22 mrad. A 45 mrad collection angle was used for EELS.

Figure 2A is a pair of HAADF and ABF images of the entire LSMO/$BaTiO_3$/LSMO thin film in the [100] orientation. The HAADF image shows a defect-free atomically abrupt LSMO/$BaTiO_3$ interface. Figure 2B is an inverted and averaged ABF image (previously interpolated (2x) and filtered) of the bottom interface with the polarization of the $BaTiO_3$ layer pointing towards the bottom interface. Figure 2C shows the Mn-O and La-O atomic intensity column profiles. The peak positions of Mn and O are determined from a Gaussian fit and we find a Mn-O *z*-displacement of 0.18 Å, 0.16 Å and 0.03 Å in the first three layers of $MnO_2$ from the bottom interface. Atomically-resolved EEL spectrum images were acquired from the LSMO/$BaTiO_3$ interfacial regions, as well as from the bulk $BaTiO_3$. Figure 2D presents the comparison between experimental and theoretical O *K*-edge EEL spectra of the Mn-O atomic columns directly adjacent to the interface showing significant changes in the fine structure of the LSMO interfacial spectra for both the polarization of the $BaTiO_3$ films (i.e. accumulation and depletion state). Figure 2E shows the pre-peak to main peak intensity ratio as a function of distance from the LSMO/$BaTiO_3$ bottom interface. Figure 2E shows that the excess of screening holes (electrons) for accumulation (depletion) decay back to bulk LSMO levels over two unit cells. [4]

References:
[1] This work is supported by the National Science Foundation [DMR-0846748]. The acquisition of the UIC JEOL JEM-ARM200CF is supported by a MRI-$R^2$ grant [DMR-0959470].

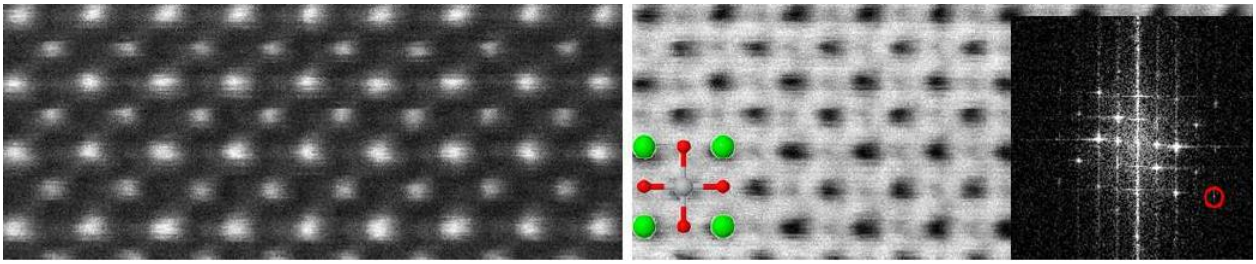

**Figure 1.** HAADF/ABF image pair acquired from the $SrTiO_3$ [100] substrate. The oxygen atomic columns are clearly visible in the ABF image. Inset: power spectrum taken demonstrating approximately 73 pm spatial resolution. A schematic of a [100] unit cell of $SrTiO_3$ is also presented (Sr - green, Ti - gray, O - red).

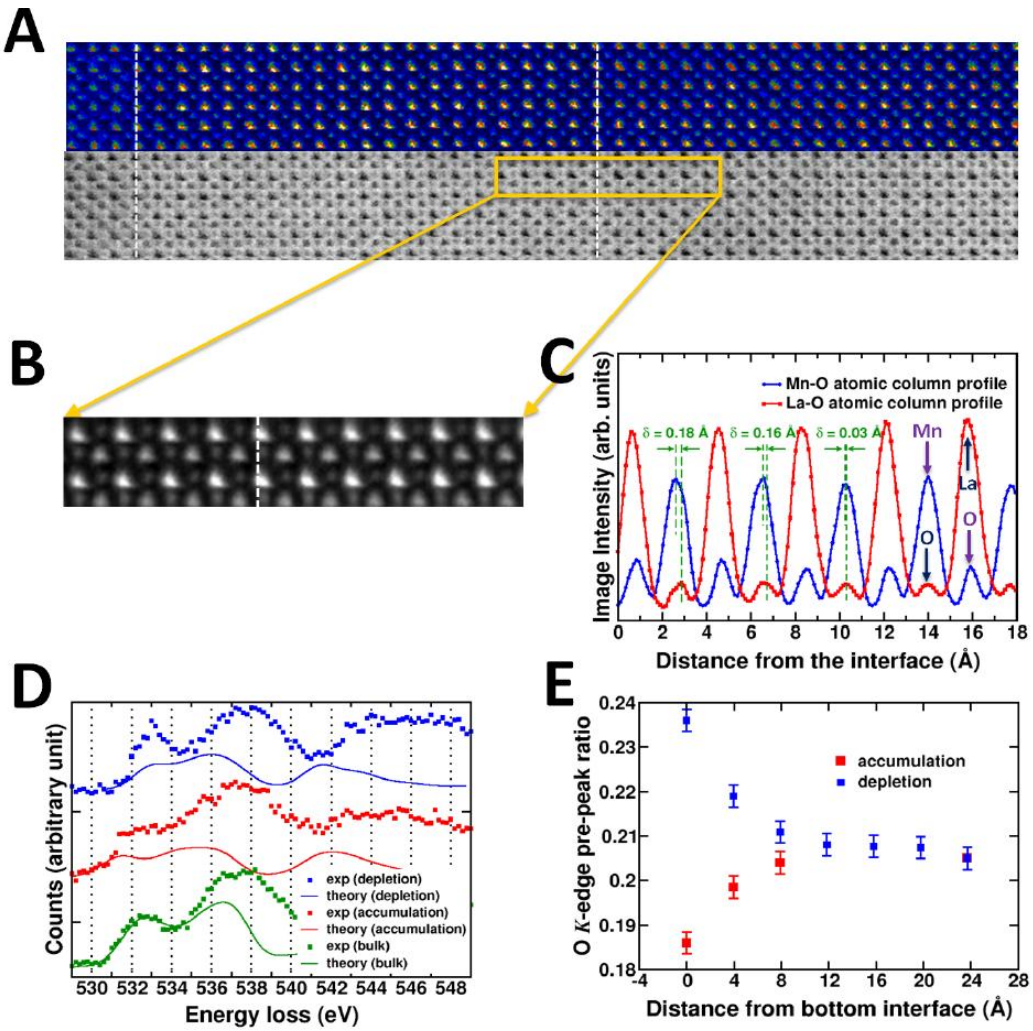


**Figure 2.** A) HAADF/ABF images of the LSMO/$BaTiO_3$/LSMO film with the interfaces marked and O columns clearly visible in ABF; B) interpolated, filtered, inverted, ABF image of the bottom interface. The apparent triangular shape of the atomic columns is an artifact of the cross-correlation and averaging process; C) intensity line profiles of the Mn-O and La-O atomic column revealing the Mn-O polarization. The higher peaks in the two curves correspond to the positions of La and Mn atoms and the lower peaks to the positions of O atoms. D) O *K*-edge EEL spectra (solid dots for experimental data and solid line for *Z*+1 simulations) of the bottom interface for each accumulation and depletion, as well as bulk LSMO; E) relative O *K*-edge pre-peak intensity as a function of position from the bottom interface.

https://doi.org/10.1017/S1431927613011975 Published online by Cambridge University Press